

Predicting ATS Open Pivot™ Heart Valve Performance with Computational Fluid Dynamics

Kris Dumont¹, Jan A. M. Vierendeels², Patrick Segers¹, Guido J. Van Nooten³, Pascal R. Verdonck¹

¹IBiTech, Institute of Biomedical Technology, ²Department of Flow, Heat and Combustion Mechanics, ³Faculty of Medicine and Health Sciences, Department of Surgery, Ghent University, Belgium

Background and aim of the study: In-vitro studies on the ATS heart valve have indicated that valve opening is less in an expanding conduit than in a straight conduit.

Methods: Bileaflet valve behavior was studied using a new computational fluid-structure interaction model. A three-dimensional model of the ATS valve was studied in two geometries, simulating the valve in a geometry with sudden expansion downstream of the valve, and in a straight conduit. Mitral and aortic flow patterns were simulated.

Results: The ATS valve in the expanding geometry showed opening to a maximum angle of 77.5°; this was confirmed in previous clinical and in-vitro studies. The mean and maximum transvalvular Doppler pressure gradients were 1.1 and 4.3 mmHg, respectively. The maximum shear stress calculated on the leaflet was 25 Pa. Maximum opening of the valve was

achieved in the straight conduit; with mean and maximum pressure gradients of 2.1 and 4.6 mmHg, respectively. The maximum shear stress calculated on the leaflet was 35 Pa.

Conclusion: The results of this numerical study confirmed that valve hemodynamics and leaflet motion were dependent on the geometrical conditions of the valve: the presence of a diverging flow influenced the maximum opening angle of the valve leaflets. This model could be used to predict pressure gradients, effective orifice area, performance index and shear stress loading of mechanical heart valves, and in future will serve as a major research tool to characterize the hemodynamics of existing and new mechanical heart valves.

The Journal of Heart Valve Disease 2005;14:393-399

Important design criteria of heart valves relate to the behavior of the valve in the flow field. In particular, pressure gradients should be as low as possible, whilst stagnation, recirculation zones (1,2) and shear stresses in the clearance region (3) should be minimized in order to prevent the initiation of coagulation.

Traditionally, the behavior of the valve (leaflets) is tested in in-vitro mock circulations (4-7), which implies that prototypes of the valves are already available at the time of testing. During the course of the design process, however, valves are computer-designed, and virtual valve prototypes are available at an early stage of the design process. However, the challenge remains to test the hemodynamic performance of these virtual prototypes. To do so, advanced computational algorithms, which take into account the continu-

ous and full interaction between the flow and the valve leaflets, are required (8-11).

Several attempts have been made to assess heart valve kinematics using numerical fluid-structure interaction (FSI) models. Peskin and McQueen (12) developed a three-dimensional model which included the heart and vessel walls and was based on the immersed boundary method. Mechanical heart valve dynamics were studied only in two dimensions using the fictitious domain method by van de Vosse et al. (13). Although these methods have the advantage that they avoid the mesh movement, they are less accurate at the interface between the blood and the leaflet. As such, shear stress values on heart valve leaflets cannot be estimated with these methods.

By using the arbitrary Lagrangian-Eulerian ALE-remeshing approach (14), shear stress values on structures such as heart valve leaflets can be estimated more accurately. There are different ways to tackle the coupled interaction problem. One possibility is to develop new software and solution methods for each of these coupled applications; this is referred to as the 'mono-

Address for correspondence:
Kris Dumont, Hydraulics Laboratory, Ghent University, Sint-Pietersnieuwstraat 41, 9000 Gent, Belgium
e-mail: kris.dumont@navier.UGent.be

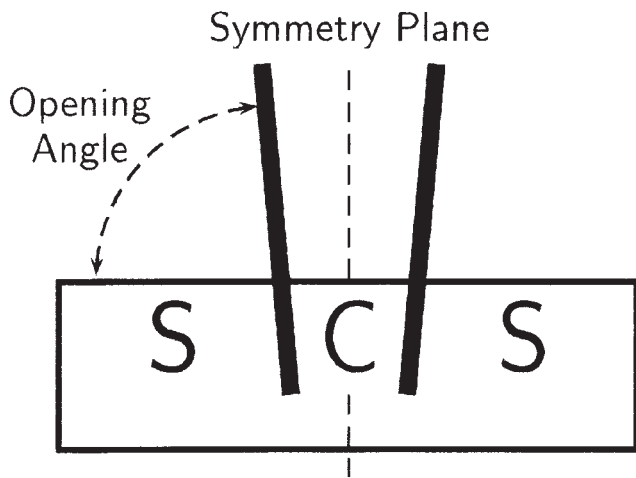


Figure 1: Opening angle, symmetry plane, side (S) and central (C) orifice of the ATS valve.

lithical approach' or the 'direct method' (15). On the other hand, one can make use of existing methods and software packages which have been developed for either fluid or structural applications and consider iterative methods (16) - also known as 'partitioned methods' (17) - for fluid-structure interaction. As such,

separate solvers are used for the fluid and the structure problem. The coupling between both, with an exchange of updated meshes and boundary conditions, is carried out in an iterative manner.

Recently, a new numerical code based on the Fluent software (Fluent, FHCI Ubanowi NH, USA) has been developed that fulfils these requirements, and validation studies have demonstrated the accuracy of these numerical simulations (10,11). This FSI code belongs to the class of partitioned, but strongly coupled, methods (10,11,18).

In the present study, this numerical code was applied to a computer model of the ATS bileaflet valve. The motivation for choosing this particular valve was based on the observation that, under certain conditions, the valve opening angle does not reach the maximum opening position (19). The results of in-vitro experiments (6,7) appear to suggest that this behavior is related to the geometrical conditions under which the valve functions: the maximum opening angle is achieved in a straight conduit, but not when the valve is placed in an expanding conduit.

In subsequent studies, the flow pattern through the ATS valve and the motion of the valve leaflets was simulated under two conditions: (i) in an expanding

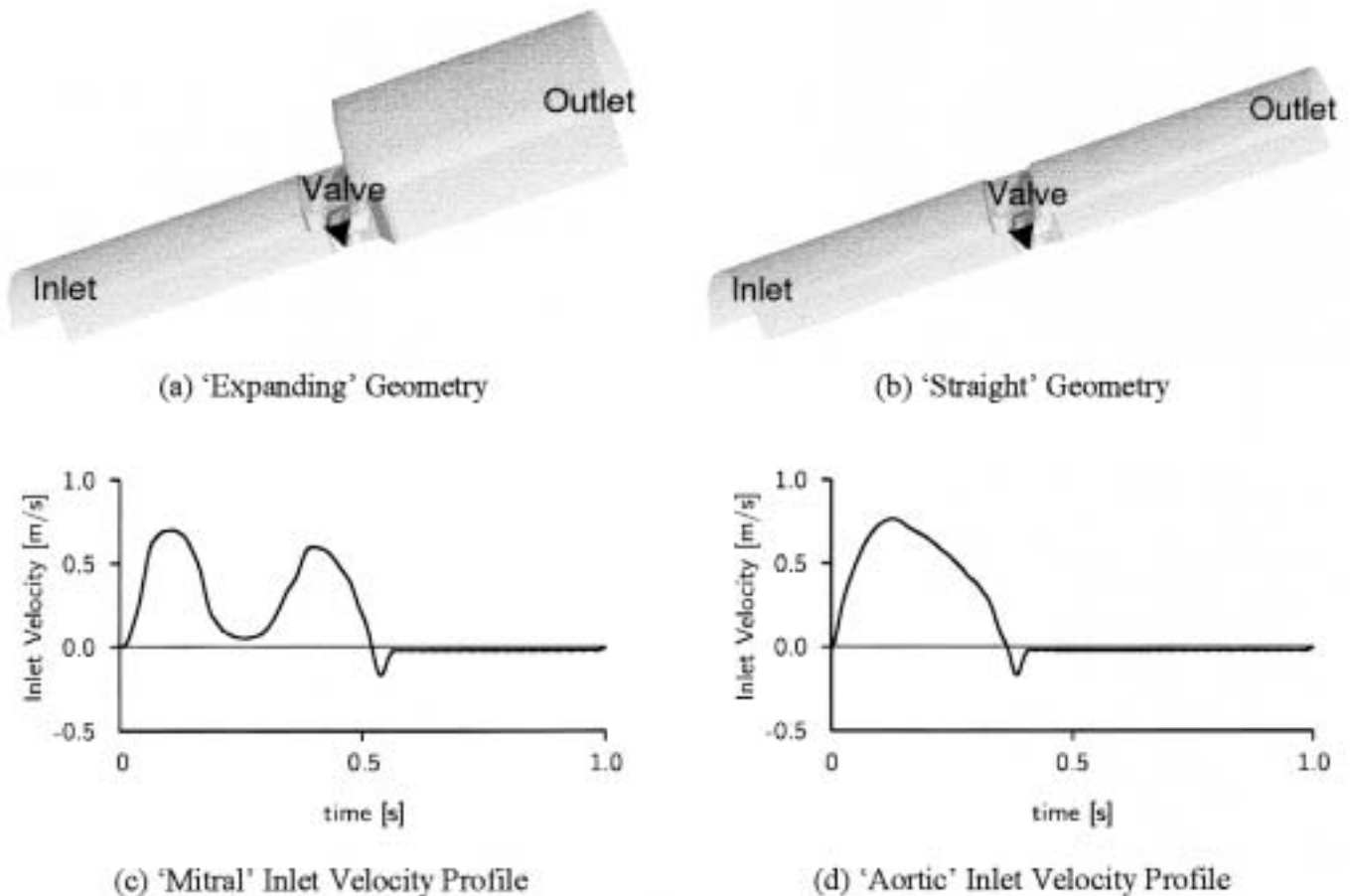


Figure 2: Studied geometries and velocity profiles.

geometry subjected to a nominal mitral flow profile; and (ii) in a straight geometry subjected to a nominal aortic flow profile. To further illustrate the possibilities of numerical simulations as 'virtual hemodynamic bench tests', the simulated data (pressure, velocity fields) were used to calculate well-known indices, which are traditionally calculated in in-vitro and clinical studies (6,7,19-21), and to characterize valve performance. This approach also allows the shear stress distribution on the valve leaflets to be calculated.

Materials and methods

Valve specifications

The model was based on the 22 mm AP ATS Open Pivot™ heart valve. The inside diameter of the valve orifice was 20.8 mm, with a geometric orifice area of 3.17 cm². Specific to this valve is its open pivot design, in which the convex pivots and stops are located on the inner circumference and extended in the flow field.

The opening angle of the leaflets and the side and central orifice of the valve are defined in Figure 1.

Geometrical and boundary conditions

Two different configurations were studied, referred to as 'straight' and 'expanding' geometries. Only one half of the valve was studied assuming symmetry of the flow. The straight geometry (Fig. 2b) is a conduit of 100 mm length and 21.9 mm diameter. The outflow conduit of the expanding geometry (Fig. 2a) was increased to 40 mm.

Inflow conditions were set 5 cm proximal to the valve. The applied flow profiles were nominal mitral and aortic flow profiles (Figs. 2c and d), with the duration of one cardiac cycle being 1 s (60 beats/min). The cardiac output for both flow profiles was 4 l/min.

Clinically relevant parameters derived from the model

Numerical simulations produce pressure and veloci-

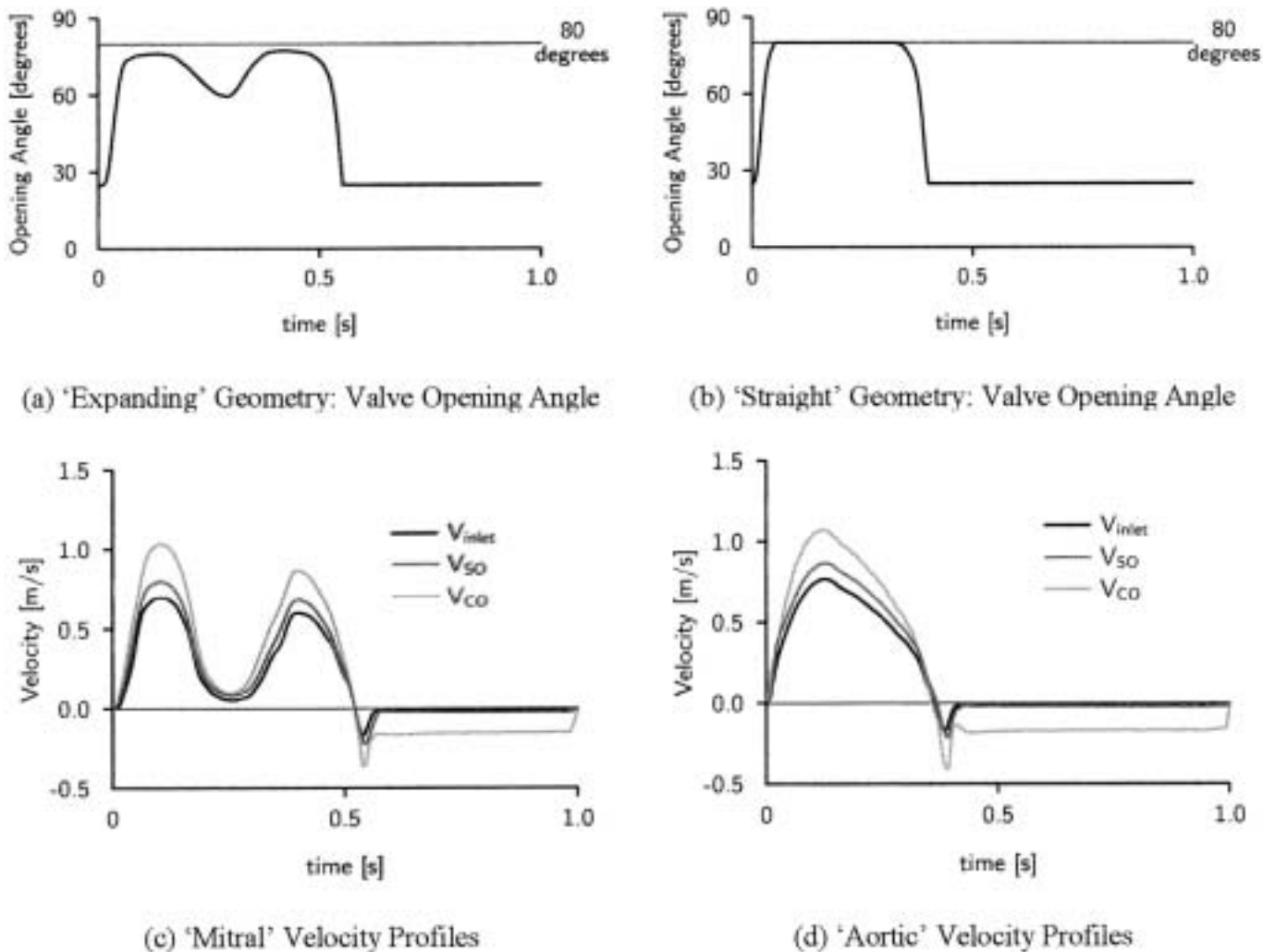


Figure 3: Valve opening angle and velocity profiles.

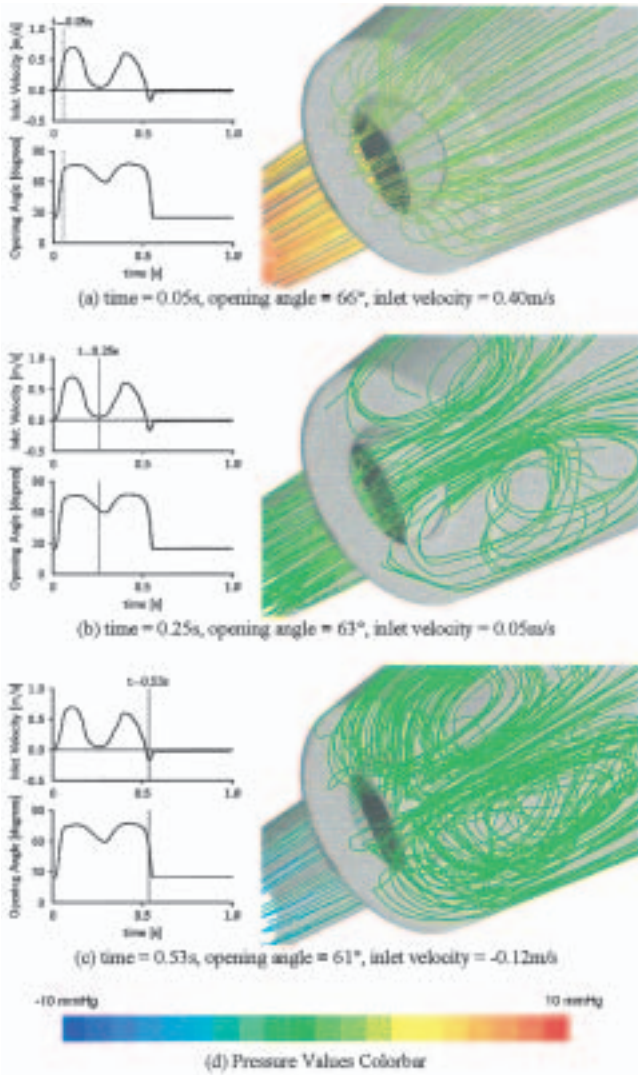


Figure 4: 'Expanding' geometry: Pathlines colored with reference to pressure.

ty in each node of the numerical grid, and the position of the valve leaflet at any moment during the cardiac cycle. With these data, it is also possible to calculate valve performance indices. The velocity in the central orifice (V_{co}) and side orifice (V_{so}), and the pressure 1.5 cm and 5 cm proximal and distal to the valve, were calculated. From these pressure data, two transvalvular pressure gradients were derived. The pressure gradient $\Delta P_{\Delta x=10 \text{ cm}}$ was defined as the pressure difference between points 5 cm proximal and distal to the valve. Likewise, the pressure gradient $\Delta P_{\Delta x=3 \text{ cm}}$ was defined as the pressure difference between points 1.5 cm proximal and distal to the valve. Mean and maximum transvalvular pressure gradients were calculated: ΔP_{mean} was the mean pressure gradient during forward flow, and ΔP_{max} the maximum pressure gradient during the cardiac cycle. In addition, the pressure

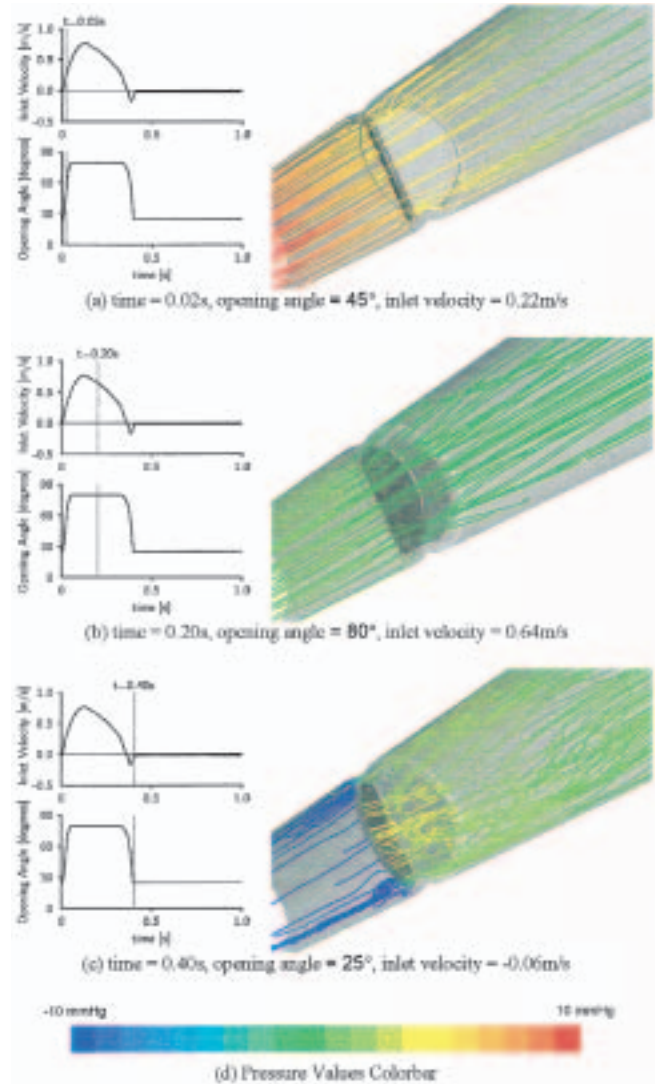


Figure 5: 'Straight' position: Pathlines colored with reference to pressure.

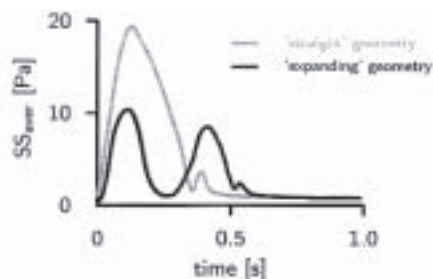
gradient ΔP_{Feng} , defined by Feng et al. (6,7) as the mean pressure difference during the acceleration phase, was calculated.

Velocity profiles were simulated at the center orifice (V_{co}) and side orifice (V_{so}) of the valve. The velocity profile at the center orifice represented the velocity that would be measured by an ultrasound machine, and was referred to here as the 'Doppler' velocity profile. The simplified Bernoulli equation was used to estimate the maximum forward pressure gradient:

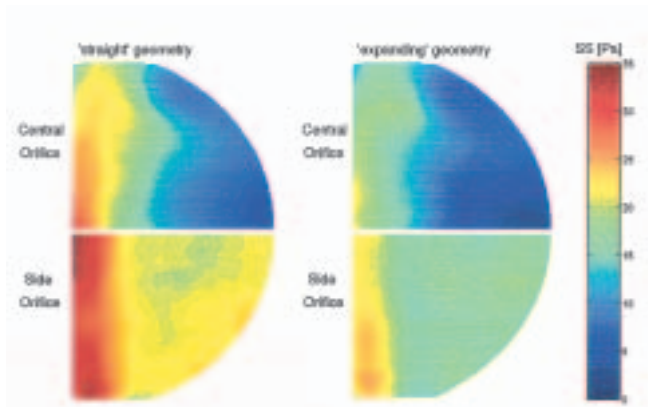
$$\Delta P_{\text{doppler, max}} = 4 \cdot V_{\text{max}}^2 \quad (1)$$

and the mean forward pressure gradient:

$$\Delta P_{\text{doppler, mean}} = 4 \cdot V_{\text{mean}}^2 \quad (2)$$



(a) SS_{avg} [Pa] on the leaflet



(b) Shear stress distribution [Pa] in the leaflet corresponding with time of max SS_{avg}

Figure 6: Shear stress (Pa) on the valve leaflets.

From the simulated velocities, it was possible to calculate the shear stress distribution on the leaflet, assuming a constant blood viscosity. Shear stress was recognized as the primary biomechanical trigger for thrombolytic and hemolytic events (22-24). From the shear stress distribution, the following were calculated:

For each time step, the spatial average shear stress on the leaflet: SS_{avg}

The time variation of SS_{avg} during the cardiac cycle with a maximum value: $maxSS_{avg}$

Maximum value of shear stress during the cardiac cycle on the leaflet: SS_{max}

Results

'Expanding' geometry

The time course of leaflet opening is illustrated diagrammatically in Figure 3(a). The valve opening angle initially reached 76.2° , moved towards a more closed position during diastasis (59.6°), and reopened during atrial contraction to an angle of 77.5° . Thus, the valve never reached the maximum opening position.

Figure 3(c) shows the velocity profiles as observed at the center orifice (V_{co}) and side orifice (V_{so}) of the valve, compared to the inlet velocity profile. V_{co} and V_{so} were then used to calculate $\Delta P_{doppler,max}$ (4.27 mmHg) and $\Delta P_{doppler,mean}$ (1.11 mmHg) (Table I). The

mean pressure gradients derived from the numerical simulations were $\Delta P_{mean,\Delta x=10\text{ cm}} = 0.49$ mmHg and $\Delta P_{mean,\Delta x=3\text{ cm}} = 0.71$ mmHg. The maximum pressure gradients derived from the numerical simulations were $\Delta P_{max,\Delta x=10\text{ cm}} = 9.20$ mmHg and $\Delta P_{max,\Delta x=3\text{ cm}} = 4.10$ mmHg. The pressure gradient ΔP_{Feng} (as defined by Feng et al.) was 2.79 mmHg.

The flow pathlines are illustrated in Figure 4, and demonstrate some of the capabilities of the numerical model. The flow pathlines diverge into the enlargement downstream of the valve (Fig. 4a and b), guiding the valve leaflet motion. Circular pathlines are furthermore present during complete closing phase of the valve (Fig. 4c).

'Straight' geometry

The valve opening with time for the straight geometry is illustrated in Figure 3b; the valve opened fully and reached the model maximum of 80° .

Figure 3d shows the velocity profiles used to calculate $\Delta P_{doppler,max}$ and $\Delta P_{doppler,mean}$ (see Table I); $\Delta P_{doppler,max}$ was 4.58 mmHg, and $\Delta P_{doppler,mean}$ 2.06 mmHg. The mean pressure gradients derived from the numerical simulations were $\Delta P_{mean,\Delta x=10\text{ cm}} = 0.70$ mmHg and $\Delta P_{mean,\Delta x=3\text{ cm}} = 0.76$ mmHg. The maximum pressure gradients derived from the numerical simulations were $\Delta P_{max,\Delta x=10\text{ cm}} = 9.79$ mmHg and $\Delta P_{max,\Delta x=3\text{ cm}} = 3.74$ mmHg. The pressure gradient ΔP_{Feng} was 3.29 mmHg.

The flow pathlines are illustrated in Figure 5; those in Figures 5a and b were more streamlined than those seen during valve closure (Fig. 5c).

Shear stress distribution

The shear stress distribution on the valve leaflet in the two geometries was calculated. The time variation of average shear stress (SS_{avg}) is shown in Figure 6a. Average shear stress (SS_{avg}) was greater in the straight geometry than in the expanding geometry (Fig. 6a). The $maxSS_{avg}$ was calculated as 10.4 Pa for the expanding geometry, and 19.3 Pa for the straight geometry. A comparison of shear stress distribution on the leaflet for the two geometries, and for the side and central ori-

Table I: Summary of hemodynamic flow and pressure data

Parameter	'Expanding' geometry	'Straight' geometry
$\Delta P_{mean,Feng}$ (mmHg)	2.79	3.29
$\Delta P_{mean,\Delta x=10\text{ cm}}$ (mmHg)	0.49	0.70
$\Delta P_{max,\Delta x=10\text{ cm}}$ (mmHg)	9.20	9.79
$\Delta P_{mean,\Delta x=3\text{ cm}}$ (mmHg)	0.71	0.76
$\Delta P_{max,\Delta x=3\text{ cm}}$ (mmHg)	4.10	3.74
$\Delta P_{doppler,mean}$ (mmHg)	1.11	2.06
$\Delta P_{doppler,max}$ (mmHg)	4.27	4.58

fice, is shown in Figure 6b (see also Fig. 1). This shear stress distribution corresponding to the time of $\max SS_{\text{avg}}$ as indicated in Figure 6a. The SS_{max} was 25 Pa for the expanding geometry, and 35 Pa for the straight geometry.

Discussion

In these studies, the ATS Open Pivot™ heart valve was simulated in two geometries, namely ‘expanding’ and ‘straight’ conduits. In both cases, a physiological inflow pattern corresponding to a cardiac output of 4 l/min was used. Although the model limitations did not allow complete simulation of forward flow across the valve, clinically relevant parameters were investigated from these numerical simulations.

Recently, a numerical code has been developed that accounts for the complex blood-leaflet interaction, and a 2D validation study has demonstrated the accuracy of the numerical simulations (10,11). Based on these observations, the algorithm was applied in a 3D setting. It is however acknowledged that further experimental measurements are required to validate the agreement between the measured and calculated complex 3D flow phenomena around the moving valve leaflet.

During forward flow conditions, the mean pressure gradients remained <3.3 mmHg for a cardiac output of 4.0 l/min, while the mean forward pressure gradients ($\Delta P_{\text{doppler, mean}}$) were 1.11 mmHg for mitral flow conditions and 2.06 mmHg for an aortic flow pattern in the respective expanding and straight geometries. These values were similar to those reported by others (25). The maximum forward pressure gradients were in good agreement with maximum pressure gradients $\Delta P_{\Delta x=3 \text{ cm}}$ for both geometries. The maximum pressure gradients $\Delta P_{\Delta x=10 \text{ cm}}$ were higher than $\Delta P_{\Delta x=3 \text{ cm}}$. In order to compare the calculated pressure gradients with published experimental data, the mean pressure gradient as defined by Feng et al. (7) was calculated; values of 2.79 and 3.29 mmHg for the expanding and straight conduits respectively compared well with Feng et al.’s value of 4.8 mmHg for the same cardiac output (7).

The impact of geometrical conditions on ATS valve leaflet motion was studied in vitro by Feng et al. (6,7), and the results confirmed the earlier findings of Aoyagi et al. (19) in the mitral position. The former authors reported less than maximum opening of the valve in an expanding conduit under mitral flow conditions, their results being in qualitative agreement with the present numerical simulations. The ATS valve in the expanding geometry showed opening to a maximum angle of 77.5° , which closely resembled the value of $75.5 \pm 1.7^\circ$ reported by Feng et al. (6,7).

Another important hemodynamic parameter, which

is impossible to measure directly either in vivo or in vitro, is that of shear stress distribution. SS_{max} on the valve leaflet was 25 Pa for the expanding geometry and 35 Pa for the straight geometry, both values being comparable with previously published data (26). The average SS_{avg} on the leaflet was 10.4 Pa in the expanding geometry, and 19.3 Pa in the straight geometry (Fig. 6a). In the former situation, the diverging flow interacts with the valve opening, thus reducing shear stress on the leaflets (see Figs. 6a and b). Thus, less than maximum opening of the valve and alignment of the leaflets with the streamlines, improves the shear stress distribution and reduces the potential for damage to platelets and blood cells.

The aim of the present study was to apply computational fluid dynamics code to a realistic 3D geometry of the ATS valve using relevant geometrical and physiological conditions. The results were found to be in qualitative agreement with previous in vivo and in vitro observations (6,7,19,25-27).

In conclusion, this numerical simulation confirms that valve hemodynamics and leaflet motion depend on the geometrical conditions of the valve: the diverging flow caused by the expanding conduit combined with the valve design characteristics led to less than maximum valve opening, but resulted in reduced shear stresses on the leaflets and reduced transvalvular pressure gradient. This computer model can be used to predict pressure gradients, shear stress distribution, and other performance indices of mechanical heart valves, and the calculated hemodynamic performances of the ATS medical valve were in agreement with published data. It is likely that this new numerical model will serve as a major research tool to characterize the hemodynamics associated with thrombolytic and hemolytic events of new and existing mechanical heart valves.

Acknowledgements

Kris Dumont is a recipient of grant IWT-SB-1117 of the Flemish Institute for the Promotion of Scientific-Technological Research in Industry.

References

1. Kelly SGD, Verdonck PR, Vierendeels JAM, Riemsdijk K, Dick E, Van Nooten GJ. A three-dimensional analysis of flow in the pivot regions of an ATS bileaflet valve. *Int J Artif Organs* 1999;22:754-763
2. Kelly SGD. Computational fluid dynamics insights in the design of mechanical heart valves. *Artif Organs* 2002;26:608-613
3. Lee CS, Chandran KB. Numerical simulation of instantaneous backflow through central clearance of bi-leaflet mechanical heart valve at closure: Shear

- stresses and pressure fields. *Med Biol Eng Comput* 1995;33:257-263
4. Verdonck P, Kleven A, Verhoeven R, Angelsen B, Vandenberghe J. Computer-controlled in vitro model of the human left heart. *Med Biol Eng Comput* 1992;30:656-659
 5. Verdonck PR, Van Nooten GJ, Van Belleghem Y. Pulse duplicator hydrodynamics of four different bileaflet valves in the mitral position. *Cardiovasc Surg* 1997;5:593-603
 6. Feng Z, Umezu M, Fujimoto T, Tsukahara T, Nurishi M, Kawaguchi D. In vitro hydrodynamic characteristics among three bileaflet valves in the mitral position. *Artif Organs* 2000;24:346-354
 7. Feng Z, Nakamura T, Fujimoto T, Umezu M. In vitro investigation of opening behavior and hydrodynamics of bileaflet valves in the mitral position. *Artif Organs* 2002;26:32-39
 8. Lai YG, Chandran KB, Lemmon J. A numerical simulation of mechanical heart valve closure fluid dynamics. *J Biomech* 2002;35:881-892
 9. Cheng R, Lai YG, Chandran KB. Two-dimensional fluid-structure interaction simulation of bileaflet mechanical heart valve flow dynamics. *J Heart Valve Dis* 2003;12:772-780
 10. Vierendeels J, Dumont K, Verdonck PR. Stabilization of a fluid-structure coupling procedure for rigid body motion. 33rd AIAA Fluid Dynamics Conference and Exhibit 2003; pages AIAA-2003-3720, 23-26 June 2003, Orlando, US
 11. Dumont K, Stijnen JMA, Vierendeels J, van de Vosse FN, Verdonck PR. Validation of a fluid-structure interaction model of a heart valve using the dynamic mesh method in fluent. *Computer Methods Biomech Biomed Eng* 2004;7:139-146
 12. Peskin CS and McQueen DM. Modeling prosthetic heart-valves for numerical-analysis of blood-flow in the heart. *J Comput Phys* 1980; 37:113-132
 13. van de Vosse F, de Hart J, van Oijen C, et al. Finite-element-based computational methods for cardiovascular fluid-structure interaction. *J Eng Math* 2003; 47:335-368
 14. Chu H. Arbitrary Lagrangian-Eulerian method for transient fluid-structure interactions. *Nucl Technol* 1980;51:363-377
 15. Blom F. A monolithical fluid-structure interaction algorithm applied to the piston problem. *Computer Methods Appl Mech Eng* 1998;167:369-391
 16. Zhang H, Bathe K. Direct and iterative computing of fluid flows fully coupled with structures. In: Bathe KJ (ed.), *Computational Fluid and Solid Mechanics*. Elsevier, Amsterdam, 2001
 17. Piperno S, Farhat C, Larrouturou B. Partitioned procedures for the transient solution of coupled aeroelastic problems: Model problem, theory and 2-dimensional application. *Computer Methods Appl Mech Eng* 1995;124:79-112
 18. Matthies H, Steindorf J. How to make weak couplings strong. In: Bathe KJ (ed.), *Computational Fluid and Solid Mechanics*. Elsevier, Amsterdam, 2001
 19. Aoyagi S, Kawara T, Fukunaga S, et al. Cineradiographic evaluation of ATS open pivot bileaflet valves. *J Heart Valve Dis* 1997;6:258-263
 20. Karpuz H, Jeanrenaud X, Hurni M, et al. Doppler echocardiographic assessment of the new ATS medical prosthetic valve in the aortic position. *Am J Cardiovasc Imaging* 1996;10:254-260
 21. Emery RW, Van Nooten GJ, Tesar PJ. The initial experience with the ATS medical mechanical cardiac valve prosthesis. *Ann Thorac Surg* 2003;75:444-452
 22. Nevaril CG, Lynch EC, Alfrey CP, Hellums JD. Erythrocyte damage and destruction induced by shearing stress. *J Lab Clin Med* 1968;71:781-790
 23. Goubergrits L, Affeld K. Numerical estimation of blood damage in artificial organs. *Int J Artif Organs* 2004;28:499-507
 24. Grigioni M, Daniele C, Morbiducci U, D'Avenio G. The power-law mathematical model for blood damage prediction: Analytical developments and physical inconsistencies. *Int J Artif Organs* 2004;28:467-475
 25. Laske A, Jenni R, Maloigne M, Vassalli G, Bertel O, Turina MI. Pressure gradients across bileaflet aortic valves by direct measurement and echocardiography. *Ann Thorac Surg* 1996;61:48-57
 26. Bluestein D, Li YM, Krukenkamp IB. Free emboli formation in the wake of bi-leaflet mechanical heart valves and the effects of implantation techniques. *J Biomech* 2002;35:1533-1540
 27. ATS Medical Inc., Pre-Market Approval Application - Summary of Safety and Effectiveness: 200. Washington DC, US Food and Drug Administration, 2000. P990046.